DALTON

Synthesis, structure and reactivity of the thioether half-sandwich rhodium(III) complex $[RhCl(MeCN)_2([9]aneS_3)][CF_3SO_3]_2$ ([9]aneS$_3$ = 1,4,7-trithiacyclononane)

Katja Brandt and William S. Sheldrick *

Lehrstuhl für Analytische Chemie, Ruhr-Universität Bochum, D-44780 Bochum, Germany

The complex $[RhCl(MeCN)_2([9]aneS_3)][CF_3SO_3]_2$ **1** ([9]aneS$_3$ = 1,4,7-trithiacyclononane) was prepared by reaction of $RhCl_3 \cdot 3H_2O$ with [9]aneS$_3$ in the presence of an excess of $Ag(O_3SCF_3)$ in acetonitrile. It has been employed as a starting material for the synthesis of the mixed-ligand sandwich complex $[Rh\{HB(pz)_3\}([9]aneS_3)][CF_3SO_3]_2$ **2** (pz = pyrazol-l-yl) and the half-sandwich complexes $[RhCl(pymt)([9]aneS_3)][CF_3SO_3]$ **3** (Hpymt = pyrimidine-2-thiolate), $[Rh(pymt)_2([9]aneS_3)][CF_3SO_3]$ **4** and $[RhCl(S_2CNEt_2)([9]aneS_3)][CF_3SO_3]$ **5**. Treatment of **1** with 2 molar equivalents of $Na[S_2CNEt_2]$ in methanol led to a base-induced ring opening of the thioether [9]aneS$_3$ and formation of the μ-S bridged dinuclear complex $[\{Rh(S_2CNEt_2)_2\}_2\{\mu\text{-}S(CH_2)_2S(CH_2)_2SCH{=}CH_2\}_2]$ **6**. The structures of **1**–**3** and **6** have been determined by X-ray crystallography.

The trithia macrocycle 1,4,7-trithiacyclononane ([9]aneS$_3$) has been successfully employed as a facially co-ordinating six-electron donor in a wide range of homoleptic complexes of lower-oxidation-state transition-metal ions.[1,2] A major motivation for the investigation of thioether co-ordination chemistry has certainly been the apparent parallel of these ligands to phosphines, since both contain large polarizable second-row elements as donor atoms. However, despite the formal analogy of the co-ordination properties of [9]aneS$_3$ to triphosphines or organometallic η^n-C_nH_n groups such as η^5-cyclopentadienyl or η^6-arene, surprisingly few studies of the synthetic potential of [9]aneS$_3$-κ^3S complexes have been reported.[3–10] We have recently described[9] the preparation and structure of the tris(acetonitrile) complex $[Ru(MeCN)_3([9]aneS_3\text{-}\kappa^3S)][CF_3SO_3]_2$, which provides an expedient starting material for the synthesis of mixed-ligand sandwich complexes such as $[Ru\{HB(pz)_3\}([9]aneS_3\text{-}\kappa^3S)][CF_3SO_3]$ (pz = pyrazol-l-yl) or dinuclear half-sandwich complexes such as $[\{Ru(\mu\text{-}S_2CNMe_2)([9]aneS_3\text{-}\kappa^3S)\}_2][CF_3SO_3]_2$.

Previous studies of [9]aneS$_3$ complexes of Rh^{III} other than the homoleptic trication $[Rh([9]aneS_3\text{-}\kappa^3S)_2]^{3+}$ are very limited. Treatment of $[Rh(C_2H_4)L([9]aneS_3\text{-}\kappa^3S)]^+$ [L = C_2H_4 or $P(C_6H_{11})_3$] with stoichiometric quantities of MeCOCl, $SiMe_3Cl$, I_2 or MeI in acetone or tetrahydrofuran (thf) at 293 K has been reported to afford yellow (for X = Cl) or orange (X = I) precipitates, which were formulated as $[RhX_3([9]aneS_3\text{-}\kappa^3S)]$ on the basis of IR spectroscopic and microanalytical data.[8] The insolubility of these products in common solvents prevented further characterization. In contrast Do and co-workers[10] have very recently isolated $[RhI_2(PPh_3)([9]aneS_3\text{-}\kappa^3S)][ClO_4]$ by the reaction of $[Rh(CO)(PPh_3)([9]aneS_3\text{-}\kappa^3S)][ClO_4]$ with a slight excess of I_2 in CH_2Cl_2. This red rhodium(III) complex was structurally characterized by X-ray analysis and employed for the preparation of the novel dinuclear compound $[([9]aneS_3\text{-}\kappa^3S)Rh(\mu\text{-}SPh)_3Rh(C_5Me_5)]^{2+}$.

In analogy to our investigations on $([9]aneS_3\text{-}\kappa^3S)Ru^{II}$ compounds we now report the preparation of $[RhCl(MeCN)_2([9]aneS_3\text{-}\kappa^3S)][CF_3SO_3]_2$ **1** and demonstrate the potential of this bis(acetontrile) derivative for the synthesis of further thioether half-sandwich complexes. Two characteristic aspects of crown thioether co-ordination chemistry will be shown to be of particular relevance for differences in the reactivity of the $([9]aneS_3\text{-}\kappa^3S)$-$Ru^{II}$ and -Rh^{III} fragments, namely the pursuit of charge neutralization and ring opening of the tridentate macrocycle in the presence of base.

Experimental

Solvents were dried and distilled before use. Proton NMR spectra were recorded on a Bruker AM-400 spectrometer, IR spectra as KBr discs on a Perkin-Elmer 1760 spectrometer and FAB mass spectra on a Fisons VG Autospec instrument employing 3-nitrobenzyl alcohol as the matrix. Elemental analyses were performed on a Carlo Erba 1106 analyser. The compound [9]aneS$_3$ was obtained from Fluka and used as received.

Syntheses

$[RhCl(MeCN)_2([9]aneS_3\text{-}\kappa^3S)][CF_3SO_3]_2$ 1. A solution of $RhCl_3 \cdot 3H_2O$ (0.263 g, 1 mmol) in MeCN (50 cm^3) was refluxed under argon for 10 h in the presence of $Ag(O_3SCF_3)$ (0.771 g, 3 mmol). After removal of AgCl by filtration a solution of [9]aneS$_3$ (0.180 g, 1 mmol) in MeCN (10 cm^3) was slowly added to the filtrate at 70 °C. The resulting solution was refluxed for 4 h, allowed to cool to ambient temperature and reduced in volume to 5 cm^3. Addition of diethyl ether (50 cm^3) followed by stirring for 3 h led to the formation of a bright-yellow precipitate which was filtered off and dried in vacuum to afford complex **1** in 86% yield (0.601 g) (Found: C, 20.2; H, 2.3; N, 3.6. $C_{12}H_{18}ClF_6N_2O_6RhS_5$ requires C, 20.6; H, 2.6; N, 4.0%). FAB mass spectrum: *m*/*z* 549 (59, $[M - CF_3SO_3]^+$), 467 (49, $[M - CF_3SO_3 - 2MeCN]^+$) and 432 (35%, $[M - CF_3SO_3 - 2MeCN - Cl]^+$). ^{1}H NMR ($CD_3OD$): δ 2.02 (6 H, s, CH_3 of MeCN) and 3.31–3.60 (12 H, m, CH_2 of [9]aneS$_3$). IR (KBr disc): $\tilde{\nu}$/cm^{-1} 2330m and 2301m (CN). Crystals for X-ray analysis were obtained by slow gas diffusion of diethyl ether into an acetonitrile solution of **1**.

$[Rh\{HB(pz)_3\text{-}\kappa^3N\}([9]aneS_3\text{-}\kappa^3S)][CF_3SO_3]_2$ 2. The salt $Na[HB(pz)_3]$ (24 mg, 0.1 mmol) was added to a solution of complex **1** (70 mg, 0.1 mmol) in MeOH (10 cm^3) and stirred for 3 h at reflux. After filtration the solvent was removed to afford **2** in 73% yield (58 mg) (Found: C, 25.0; H, 2.5; N, 10.0. $C_{17}H_{22}BF_6N_6O_6RhS_5$ requires C, 25.7; H, 2.8; N, 10.6%). FAB mass spectrum: *m*/*z* 645 (9, $[M - CF_3SO_3]^+$) and 496

(100%, $[M - 2CF_3SO_3]^+$). ^1H NMR (CD_3OD): δ 3.80 (6 H, m, CH_2 of [9]aneS_3), 4.02 (6 H, m, CH_2 of [9]aneS_3), 6.59 (3 H, dd, H^4 of pz), 7.97 (3 H, d, J = 2.4, H^3 or H^5 of pz) and 8.17 (3 H, d, J = 2.4 Hz, H^3 or H^5 of pz). IR (KBr disc): $\tilde{\nu}/cm^{-1}$ 2524m (BH). Recrystallization from methanol–diethyl ether solution yielded suitable crystals for X-ray analysis.

[RhCl(pymt)([9]aneS_3-κ^3S)][CF_3SO_3] 3. Pyrimidine-2-thiolate (Hpymt) (22 mg, 0.2 mmol) was dissolved in MeOH (3 cm^3) by addition of 1 mol dm^3 methanolic NaOMe (0.2 cm^3). The subsequent solution was refluxed for 3 h with complex **1** (140 mg, 0.2 mmol) in MeOH (10 cm^3). After cooling to room temperature and filtration, slow evaporation of the filtrate provided orange crystals of **3** in 79% yield (91 mg) (Found: C, 22.8; H, 2.5; N, 4.8. $C_{11}H_{15}ClF_3N_2O_3RhS_5$ requires C, 22.8; H, 2.6; N, 4.8%). FAB mass spectrum: m/z 429 (80, $[M - CF_3SO_3]^+$) and 394 (19%, $[M - CF_3SO_3 - Cl]^+$). ^1H NMR [$(CD_3)_2SO$]: δ 3.10–3.58 (12 H, m, CH_2 of [9]aneS_3), 7.20 (1 H, t, H^5 of pymt), 8.67 (1 H, dd, H^4 or H^6 of pymt) and 8.74 (1 H, m, H^4 or H^6 of pymt). Recrystallization from acetonitrile–diethyl ether yielded crystals for X-ray analysis.

[Rh(pymt)$_2$([9]aneS_3-κ^3S)][CF_3SO_3] 4. Pyrimidine-2-thiolate (Hpymt) (45 mg, 0.4 mmol) was dissolved in MeOH (3 cm^3) by addition of 1 mol dm^3 methanolic NaOMe (0.4 cm^3). The resulting solution was refluxed for 3 h with complex **1** (140 mg, 0.2 mmol) in MeOH (10 cm^3). After cooling and filtration, **4** was separated as the major product in 62% yield (81 mg) by use of column chromatography (Sephadex LH-20, eluent MeOH) (Found: C, 27.6; H, 2.7; N, 9.1. $C_{15}H_{18}F_3N_4O_3RhS_6$ requires C, 27.5; H, 2.8; N, 8.6%). FAB mass spectrum: m/z 505 (100, $[M - CF_3SO_3]^+$) and 394 (58%, $[M - CF_3SO_3 - pymt]^+$). ^1H NMR (CD_3CN): δ 2.75–3.52 (12 H, m, CH_2 of [9]aneS_3), 6.90, 7.00 (2 H, 2t, H^5 of pymt), 8.33 (2 H, d, H^4 and H^6 of pymt-κS), 8.46 (1 H, m, H^4 or H^6 of pymt-κ$^2N,S$) and 8.53 (1 H, dd, H^4 or H^6 of pymt-κ$^2N,S$).

[RhCl(S_2CNEt_2)([9]aneS_3-κ^3S)][CF_3SO_3] 5. A solution of complex **1** (140 mg, 0.2 mmol) in MeOH (15 cm^3) was refluxed with Na[S_2CNEt_2]·3H_2O (45 mg, 0.2 mmol) for 3 h. After cooling and filtration, orange **5** was separated as the major product in 85% yield (105 mg) by use of column chromatography (Sephadex LH-20, eluent MeOH) (Found: C, 22.7; H, 3.4; N, 2.2. $C_{12}H_{22}ClF_3NO_3RhS_6$ requires C, 23.4; H, 3.6; N, 2.3%). FAB mass spectrum: m/z 466 (100, $[M - CF_3SO_3]^+$) and 431 (23%, $[M - CF_3SO_3 - Cl]^+$). ^1H NMR (CD_3CN): δ 1.27 (6 H, t, CH_3 of S_2CNEt_2), 3.04–3.38 (12 H, m, CH_2 of [9]aneS_3) and 3.71 (4 H, 2 q, CH_2 of S_2CNEt_2).

[{Rh(S_2CNEt_2)$_2$}$_2${μ-S(CH_2)$_2$S(CH_2)$_2$SCH=CH_2}$_2$] 6. Complex **1** (105 mg, 0.15 mmol) was refluxed with Na[S_2CNEt_2]·3H_2O (68 mg, 0.3 mmol) for 3 h in MeOH (20 cm^3). After cooling and filtration, red **6** was separated as the major product in 72% yield (125 mg) by use of column chromatography (Sephadex LH-20, eluent MeOH) (Found: C, 32.1; H, 5.3; N, 4.4. $C_{32}H_{62}N_4Rh_2S_{14}$ requires C, 33.2; H, 5.4; N, 4.8%). FAB mass spectrum: m/z 1156 (7, M^+), 1008 (9, $[M - S_2CNEt_2]^+$), 977 (23, $[M - S_3C_6H_{11}]^+$), 829 (4, $[M - S_2CNEt_2 - S_3C_6H_{11}]^+$), 578 (28, $[M - \{Rh(S_2CNEt_2)_2(S_3C_6H_{11})\}]^+$), and 430 (100%, $[M - \{Rh(S_2CNEt_2)_2(S_3C_6H_{11})\} - S_2CNEt_2]^+$). ^1H NMR (CD_3OD): δ 1.34 (24 H, m, CH_3 of S_2CNEt_2), 2.73–3.50 (16 H, m, CH_2 of $S_3C_6H_{11}$), 3.79 (16 H, m, CH_2 of S_2CNEt_2), 5.23 (4 H, m, CH=CH_2 of $S_3C_6H_{11}$) and 6.44 (2 H, m, CH=CH_2 of $S_3C_6H_{11}$). Crystals for X-ray analysis were grown by slow evaporation of a methanol solution.

X-Ray crystallography

Crystal and refinement data for the complexes **1–3** and **6** are provided in Table 3. Diffracted intensities were collected on a Siemens P4 four-circle diffractometer in the ω-scan mode for **1–3** and in the θ–2θ scan mode for **6** with graphite-monochromated Mo-Kα radiation (λ = 0.710 73 Å) at 293 K. In each case three control intensities were monitored after collection of 100 reflections; no significant alterations in their intensities were registered. Semiempirical absorption corrections were applied on the basis of ψ-scan data. The structures were solved by a combination of Patterson and Fourier-difference syntheses and refined by full-matrix least squares against F for **1–3**[11] and against F^2 for **6**.[12] A degree of disorder was established for the carbon atoms C(21)/C(21′) and C(22)/C(22′) of the second acetonitrile ligand in complex **1**. These were refined with site occupation factors (s.o.f.s) 0.80/0.20 and bond-length constraints for N(2)–C(21)/C(21′) and C(21)/C(21′)–C(22)/C(22′). A corresponding disorder is also observed for the second $CF_3SO_3^-$ anion in the crystal lattice of **1**. Whereas all atoms of the preferred anion siting (s.o.f. 0.80) could be localized and refined, this was only the case for S(22′) of the less-preferred anion siting (s.o.f. 0.20). Anisotropic thermal parameters were introduced for the non-disordered atoms and S(21′). The facially co-ordinated [9]aneS_3 in [Rh{HB(pz)$_3$-κ^3N}([9]aneS_3-κ^3S)]$^{2+}$ **2** is disordered about a crystallographic mirror plane. The carbon atoms C(21)–C(52) of the thioether possess s.o.f.s of 0.50 and were refined with constraints for their C–C and C–S bonds. One pyrazole ring of HB(pz)$_3$ and the atoms Rh and S(1) are sited on the mirror plane at x = 0.0. Thus one conformation of the [9]aneS_3 ligand contains C(21), C(31), C(51) and the symmetry-related positions C(52a), C(32a), C(22a), the second contains C(22), C(32), C(52) and the symmetry-related positions C(51a), C(31a), C(21a). Rotational disorder about the S–C bond is observed for the second $CF_3SO_3^-$ anion, the relevant s.o.f.s being 0.58 for O(51), O(52), F(51) and F(52) and 0.42 for O(41), O(42), F(41) and F(42). Anisotropic thermal parameters were refined for the non-disordered atoms in **2**; hydrogen atoms were included at calculated positions for the pyrazole rings of the HB(pz)$_3$ ligand of the cation. Rotational disorder is once again exhibited by the $CF_3SO_3^-$ anion in **3** with s.o.f.s of 0.50 for the individual oxygen and fluorine atoms. All non-disordered atoms were assigned anisotropic thermal parameters, hydrogen-atom sites were calculated geometrically for the [9]aneS_3 and pyrimidine-2-thiolate ligands of the cation. The long-chain ethene thiolate ligands $[S(CH_2)_2S(CH_2)_2SCH{=}CH_2]^-$ in **6** display severe disordering with s.o.f.s of 0.5 for the carbon atoms C(2)–C(5) and S(10) in the central part of the chain and 0.25 for the terminal atoms C(61)/C(62) and C(61′)/C(62′). As for the other complexes, anisotropic thermal parameters were refined for the non-disordered atoms; hydrogen atoms were included at calculated sites for the diethyldithiocarbamate ligands. Complex **6** displays crystallographic C_i symmetry. Final R factors are listed in Table 3 with weighting schemes $w^{-1} = [\sigma^2(F_o) + g|F_o|^2]$ for $R' = [\Sigma w(|F_o| - |F_c|)^2/\Sigma w|F_o|^2]^{\frac{1}{2}}$ for **1–3**. For the refinement against F^2 in **6**, $w^{-1} = [\sigma^2(F_o^2) + (0.0923P)^2 + 145.68P]$, where $P = [\max(F_o^2, 0) + 2F_c^2]/3$ for $wR2 = [\Sigma w(F_o^2 - F_c^2)^2/\Sigma w(F_o^2)^2]^{\frac{1}{2}}$. Scattering factors and corrections for anomalous dispersion were taken from ref. 13. Fractional atomic coordinates for the refined crystal structures are listed in Table 4, selected bond lengths and angles in Tables 1 and 2.

Complete atomic coordinates, thermal parameters and bond lengths and angles have been deposited at the Cambridge Crystallographic Data Centre. See Instructions for Authors, *J. Chem. Soc., Dalton Trans.*, 1996, Issue 1.

Results and Discussion

Treatment of $RhCl_3$·3H_2O with 3 equivalents of Ag(O_3SCF_3) in refluxing acetonitrile followed by filtration of AgCl and addition of an equivalent of [9]aneS_3 provides the novel

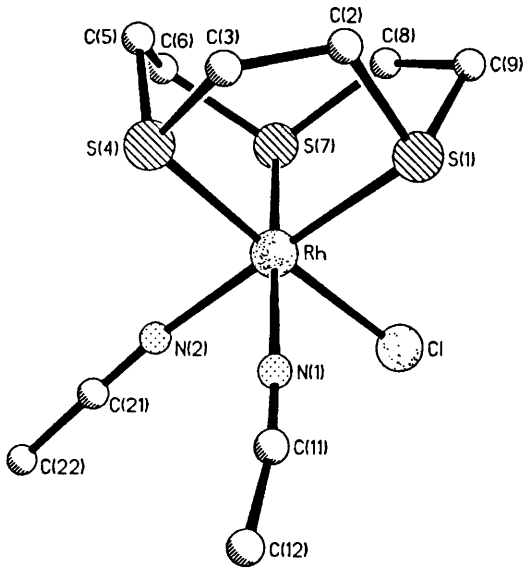

Fig. 1 Molecular structure of the cation $[RhCl(MeCN)_2([9]aneS_3\text{-}\kappa^3S)]^{2+}$ **1**

Table 1 Selected bond lengths (Å) for complexes **1**–**3** and **6** with estimated standard deviations (e.s.d.s) in parentheses

Compound **1**			
Rh–Cl	2.337(5)	Rh–S(1)	2.264(14)
Rh–S(4)	2.287(4)	Rh–S(7)	2.239(15)
Rh–N(1)	2.06(2)	Rh–N(2)	2.07(2)
Compound **2**			
Rh–S(1)	2.296(3)	Rh–S(4)	2.290(3)
Rh–N(11)	2.089(7)	Rh–N(21)	2.083(10)
N(11)–N(12)	1.370(9)	N(21)–N(22)	1.347(14)
Compound **3**			
Rh–Cl	2.355(3)	Rh–S(1)	2.278(3)
Rh–S(4)	2.270(4)	Rh–S(7)	2.311(3)
Rh–S(11)	2.387(3)	Rh–N(11)	2.070(9)
S(11)–C(11)	1.736(15)	C(11)–N(11)	1.339(15)
Compound **6**			
Rh–S(11)	2.360(4)	Rh–S(21)	2.360(4)
Rh–S(12)	2.369(4)	Rh–S(22)	2.375(4)
Rh–S(8)	2.350(3)	Rh–S(8a)	2.359(4)
S(11)–C(11)	1.70(1)	S(21)–C(21)	1.71(2)
S(12)–C(12)	1.73(1)	S(22)–C(22)	1.72(2)

bis(acetonitrile) complex $[RhCl(MeCN)_2([9]aneS_3\text{-}\kappa^3S)][CF_3SO_3]_2$ **1** which, in analogy to $[Ru(MeCN)_3([9]aneS_3\text{-}\kappa^3S)][CF_3SO_3]_2$, proves to be a useful starting material for the synthesis of half-sandwich complexes. Substitution of the last chloride ligand by a third acetonitrile ligand cannot be achieved under these conditions, even in the presence of a large molar excess of $Ag(O_3SCF_3)$ (6:1). This is in accordance with the well documented[14–16] restricted ability of thioethers to neutralize positive charge through σ donation. Complex **1** was characterized by FAB mass and ^1H NMR spectroscopy and by X-ray structural analysis (Fig. 1). The observation of a ^1H NMR signal at δ 2.02 is typical for co-ordinated acetonitrile ligands. The atoms of the octahedral rhodium(III) co-ordination sphere (N,S,Cl) in the crystal lattice of **1** conform to a pseudo-crystallographic mirror plane, which does not apply to the carbon atoms of the chiral five-membered chelate rings. The Rogers η factor[17] refined to 0.73(10) for the configuration of the five-membered chelate rings depicted in Fig. 1. As may be discerned from Table 2, the angle deviations from an idealized octahedron are relatively

Table 2 Selected bond angles (°) with e.s.d.s in parentheses

Compound **1**			
Cl–Rh–S(1)	87.6(6)	Cl–Rh–S(4)	176.0(5)
S(1)–Rh–S(4)	88.4(4)	Cl–Rh–S(7)	88.5(6)
S(1)–Rh–S(7)	90.1(5)	S(4)–Rh–S(7)	91.0(4)
Cl–Rh–N(1)	88.2(9)	S(1)–Rh–N(1)	89.3(8)
S(4)–Rh–N(1)	92.2(8)	S(7)–Rh–N(1)	176.7(9)
Cl–Rh–N(2)	95.5(9)	S(1)–Rh–N(2)	176.2(9)
S(4)–Rh–N(2)	88.5(8)	S(7)–Rh–N(2)	92.1(8)
N(1)–Rh–N(2)	88.7(10)		
Compound **2**			
S(1)–Rh–S(4)	89.0(1)	S(4)–Rh–S(4a)	89.4(1)
S(1)–Rh–N(11)	92.5(2)	S(1)–Rh–N(21)	179.6(3)
S(4)–Rh–N(11)	92.7(2)	S(4)–Rh–N(11a)	177.4(2)
S(4)–Rh–N(21)	90.7(2)	N(11)–Rh–N(11a)	85.2(4)
N(11)–Rh–N(21)	87.8(3)	Rh–N(21)–N(22)	118.2(7)
Rh–N(11)–N(12)	117.3(6)		
Compound **3**			
Cl–Rh–S(1)	177.3(1)	Cl–Rh–S(4)	90.3(1)
S(1)–Rh–S(4)	90.6(1)	Cl–Rh–S(7)	87.9(1)
S(1)–Rh–S(7)	89.6(1)	S(4)–Rh–S(7)	89.5(1)
Cl–Rh–S(11)	92.0(1)	S(1)–Rh–S(11)	90.4(1)
S(4)–Rh–S(11)	100.6(1)	S(7)–Rh–S(11)	169.9(1)
Cl–Rh–N(11)	90.9(2)	S(1)–Rh–N(11)	88.8(2)
S(4)–Rh–N(11)	168.9(3)	S(7)–Rh–N(11)	101.6(3)
S(11)–Rh–N(11)	68.3(3)	Rh–S(11)–C(11)	80.1(4)
Rh–N(11)–C(11)	102.5(8)	N(11)–C(11)–S(11)	109.1(9)
Compound **6**			
S(8)–Rh–S(8a)	83.1(1)	S(8)–Rh–S(11)	172.8(1)
S(8)–Rh–S(12)	100.5(1)	S(8)–Rh–S(21)	91.0(1)
S(8)–Rh–S(22)	92.4(1)	S(8a)–Rh–S(11)	92.5(1)
S(8a)–Rh–S(12)	89.1(1)	S(8a)–Rh–S(21)	101.3(1)
S(8a)–Rh–S(22)	173.1(1)	S(11)–Rh–S(12)	73.6(1)
S(11)–Rh–S(21)	95.5(1)	S(11)–Rh–S(22)	92.4(2)
S(12)–Rh–S(21)	165.4(1)	S(12)–Rh–S(22)	96.9(2)
S(21)–Rh–S(22)	73.6(2)	Rh–S(8)–Rh(a)	96.9(1)
Rh–S(11)–C(11)	87.8(5)	Rh–S(21)–C(21)	87.8(6)
Rh–S(12)–C(11)	86.7(4)	Rh–S(22)–C(21)	87.1(6)
S(11)–C(11)–S(12)	111.8(7)	S(21)–C(21)–S(22)	111.5(9)

small, with average S–Rh–S angles of 89.8°. A marked deviation from linearity is observed for the Rh–N–C angles in both of the co-ordinated acetonitrile ligands. The relevant angles are 172(3)° for N(1) and 167(3) or 166(3)° for N(2) in the disordered positions of the second acetonitrile.

In analogy to our previous report[9] on $[Ru(MeCN)_3([9]aneS_3\text{-}\kappa^3S)][CF_3SO_3]_2$, we investigated the synthetic potential of complex **1** by studying its reactions with the potentially tridentate ligands $HB(pz)_3^-$, pyrimidine-2-thiolate ($pymt^-$) and $S_2CNEt_2^-$. Refluxing a methanol solution of **1** with $Na[HB(pz)_3]$ leads to formation of the mixed-sandwich complex $[Rh\{HB(pz)_3\text{-}\kappa^3N\}([9]aneS_3\text{-}\kappa^3S)][CF_3SO_3]_2$ **2**, which can be recrystallized from a methanol–diethyl ether solution to afford crystals suitable for a X-ray analysis (Fig. 2). Complex **2** exhibits peaks at m/z = 645 and 496 in its FAB mass spectrum, which may be assigned to the molecular ions $[M - CF_3SO_3]^+$ and $[M - 2CF_3SO_3]^+$. On the basis of its proton NMR spectrum in CD_3OD, the complex cation of **2** displays C_{3v} symmetry in solution. Only two multiplets are observed at δ 3.80 and 4.02 for the CH_2 protons of the co-ordinated thioether and three signals for the aromatic protons of the equivalent pyrazolyl protons. Whereas an overlapping doublet of doublets at δ 6.59 can immediately be assigned to the central H^4 pyrazolyl protons, a clear distinction between H^3 (the proton closest to the rhodium atom) and H^5 is not possible. Trofimenko[18] observed that the resonance with the largest coupling constant for $HB(pz)_3^-$ was consistently more sensitive to changes in metal binding. This led him to conclude that this signal belongs to H^3, the proton closest to the pyrazolyl

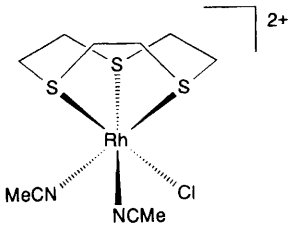

1

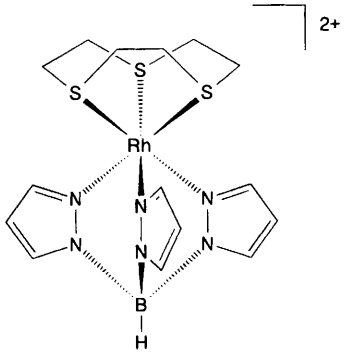

2

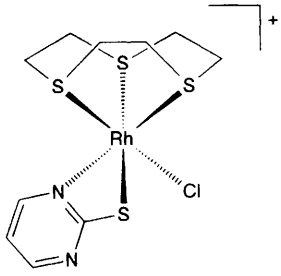

3

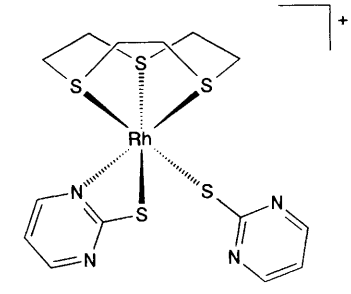

4

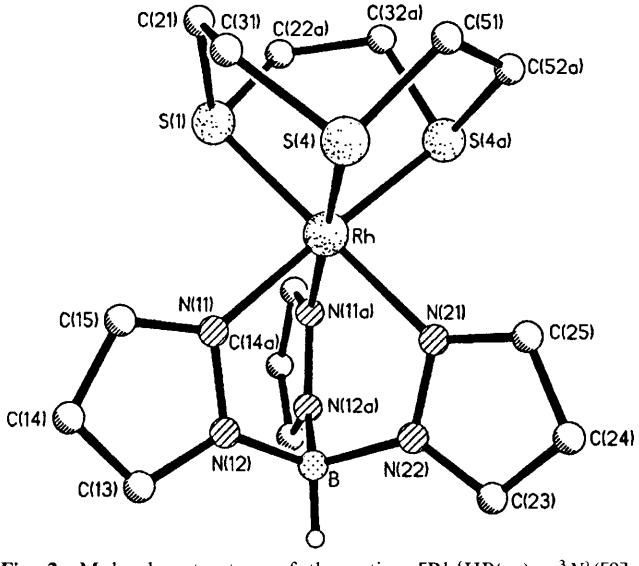

Fig. 2 Molecular structure of the cation $[Rh\{HB(pz)_3\text{-}\kappa^3N\}([9]aneS_3\text{-}\kappa^3S)]^{2+}$ **2**. The positions C(22a), C(32a) and C(52a) belonging to the depicted [9]$aneS_3$ ligand are generated from the disordered sites C(22), C(32) and C(52) by the crystallographic mirror plane

nitrogen co-ordinated to the metal. Using this argument, Mann and co-workers[19] assigned the doublet at δ 7.63 for $[Ru(\eta^5\text{-}C_5H_5)\{HB(pz)_3\text{-}\kappa^3N\}]^+$ to H^3 and that at δ 8.12 to H^5. An analogous assignment for **2** cannot be performed on this basis, as the doublets at δ 7.97 and 8.17 exhibit identical coupling constants. The B–H stretching mode gives rise to an IR band at 2524 cm^{-1}, about 70 cm^{-1} higher than that for the corresponding band of the free anion, in good agreement with data from other pyrazolylborate complexes.[19,20] Whereas the N–Rh–N angles from the κ^3N co-ordinated $HB(pz)_3^-$ ligand are markedly smaller than the idealized octahedral angle [85.2(4), 87.8(3)°], only a marginal degree of narrowing is observed for the κ^3S co-ordinated [9]$aneS_3$ ligand [89.0(1), 89.4(1)°]. The Rh–S distances in **2** [2.290(3), 2.296(3) Å] are significantly shorter than the average values of 2.341(6) Å in $[Rh([9]aneS_3\text{-}\kappa^3S)_2][CF_3SO_3]_3$ and 2.340(7) Å in $[Rh(\eta^5\text{-}C_5Me_5)([9]aneS_3\text{-}\kappa^3S)][ClO_4]_2$.[21,22] The latter compound, which was prepared by the reaction of $[Rh(\eta^5\text{-}C_5Me_5)(MeCN)_3][ClO_4]_2$ with [9]$aneS_3$ in acetonitrile,[22] provides the only previous example of a heteroleptic ([9]$aneS_3$)Rh^{III} sandwich complex.

Treatment of $[Ru(MeCN)_3([9]aneS_3\text{-}\kappa^3S)][CF_3SO_3]_2$ with $Na[S_2CNMe_2]$[9] or the anions of the heterocyclic thioamides 2-sulfanylbenzothiazole (Hbtt)[23] and 2-sulfanylpyridine (Hpyt)[23] yields dinuclear complexes of the type $[\{Ru([9]aneS_3\text{-}\kappa^3S)\}_2(\mu\text{-}L)_2][CF_3SO_3]_2$ (L = $S_2CNMe_2^-$, btt^- or pyt^-), which contain tridentate bridging ligands and a central four-membered $(RuS)_2$ ring. It was, therefore, of interest to establish whether analogous complex cations $[\{Rh([9]aneS_3\text{-}\kappa^3S)\}_2(\mu\text{-}L)_2]^{4+}$ can be prepared for the ([9]$aneS_3$-κ^3S)Rh^{III} fragment. The limited ability of the macrocyclic thioether to neutralize the high positive charge on the individual Rh atoms in such dinuclear species would suggest that this should not be expected and this hypothesis is confirmed by our experimental findings. Treatment of **1** with the anions $pymt^-$ or $S_2CNEt_2^-$ in a 1:1 molar ratio affords only the monomeric complexes $[RhCl(pymt)([9]aneS_3\text{-}\kappa^3S)][CF_3SO_3]$ **3** and $[RhCl(S_2CNEt_2)([9]aneS_3\text{-}\kappa^3S)][CF_3SO_3]$ **5**, in which the chloride ligand remains co-ordinated to enable a higher degree of charge neutralization. Peaks at m/z = 429 and 394 in the FAB mass spectrum of **3** may be assigned to the molecular ions $[M - CF_3SO_3]^+$ and $[M - CF_3SO_3 - Cl]^+$. The resonance at δ 7.20 in the ^1H NMR spectrum belongs to the central pyrimidine proton H^5, those at lower field (δ 8.67, 8.74) to the protons adjacent to pyrimidine nitrogen atoms. The structure of the cation as determined by X-ray analysis is depicted in Fig. 3. A pronounced *trans* influence is apparent in the dimensions of the distorted-octahedral co-ordination sphere of the rhodium atom, with the Rh–S(7) bond [*trans* to Rh–S(11)] being markedly longer [2.311(3) Å] than the Rh–S bonds *trans* to Cl [2.278(3) Å] and N(11) [2.270(4) Å]. Competitive π-back bonding to the *trans*-sited sulfur atom S(11) is presumably responsible for the weakening of the Rh–S(7) bond to the macrocyclic thioether. The S(11)–C(11) distance of 1.736(15) Å is in accordance with a predominantly thiolate formulation of the chelating pymt ligand.[24,25]

Reaction of complex **1** with $pymt^-$ in 1:2 molar ratio affords $[Rh(pymt)_2([9]aneS_3\text{-}\kappa^3S)][CF_3SO_3]$ **4** as the major product (62% yield). The FAB mass spectrum contains peaks at m/z =

Table 3 Crystal and refinement data for complexes **1**–**3** and **6**

	1	**2**	**3**	**6**
Formula	$C_{12}H_{18}ClF_6N_2O_6RhS_5$	$C_{17}H_{22}BF_6N_6O_6RhS_5$	$C_{11}H_{15}ClF_3N_2O_3RhS_5$	$C_{32}H_{62}N_4Rh_2S_{14}$
M (g mol^{-1})	698.9	794.4	578.9	1157.5
Crystal system	Monoclinic	Orthorhombic	Monoclinic	Hexagonal
Space group	$P2_1$	*Cmca*	$P2_1/n$	$R\bar{3}$
a/Å	10.909(4)	10.181(2)	11.785(2)	33.557(5)
b/Å	10.642(4)	26.609(4)	11.987(2)	33.557(5)
c/Å	11.463(5)	22.194(4)	14.614(3)	11.850(2)
β/°	109.76(3)	90	109.07(3)	90
U/Å^3	1252.4(9)	6012(2)	1951.3(6)	11 556(3)
Z	2	8	4	9
D_c/g cm^{-3}	1.853	1.755	1.971	1.497
F(000)	696	3184	1152	5364
Crystal size/mm	0.29 × 0.32 × 0.54	0.15 × 0.46 × 0.48	0.22 × 0.24 × 0.59	0.16 × 0.17 × 0.62
μ(Mo-Kα)/mm^{-1}	1.28	1.00	1.59	1.24
Scan width/°	1.20	1.20	1.20	2.50
$2\theta_{max}$/°	50	55	50	45
hkl Ranges	−12 to 0, −12 to 0, −12 to 13	0–13, 0–34, 0–28	0–15, −15 to 0, −18 to 18	0–31, 0–31, −12 to 12
Transmission (maximum, minimum)	0.38, 0.31	0.39, 0.35	0.27, 0.21	0.47, 0.41
Reflections collected	2452	3784	3763	3555
Independent reflections	2321	3618	3400	3351
R_{int}	0.015	0.034	0.014	0.039
Observed reflections [$I > \sigma(I)$]	1754	2171	2128	1929
No. parameters	255	215	228	238
R	0.067	0.071	0.061	0.071 [$I > 2\sigma(I)$]
R'	0.063	0.070	0.060	0.219[a] (all data)
g In weighting scheme	0.0	0.0001	0.000 05	[b]
ΔF Synthesis (maximum, minimum)/e Å^{-3}	1.11, −0.55	1.22, −0.78	1.00, −1.08	1.10, −0.82

[a] $wR2$ for refinement against F^2. [b] See text.

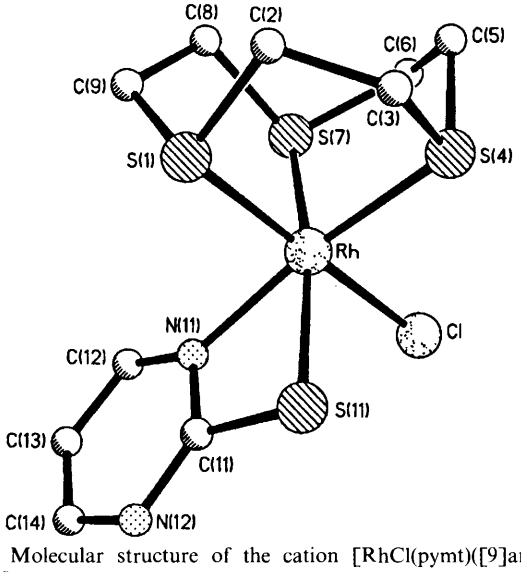

Fig. 3 Molecular structure of the cation [RhCl(pymt)([9]aneS$_3$-κ^3*S*)]$^+$ **3**

505 and 394, which belong to the molecular ions [M − CF_3SO_3]$^+$ and [M − CF_3SO_3 − pymt]$^+$ for this mononuclear complex. Two sets of ^{1}H NMR signals correspond to the aromatic pyrimidine protons of the non-equivalent pymt$^-$ ligands in **4**, which must display differing κ*S* and κ^2*N*,*S* co-ordination modes. The H^4 and H^6 protons adjacent to ring nitrogens are magnetically equivalent in the κ*S* mode and produce a doublet at δ 8.33. In contrast, these protons are non-equivalent for the κ^2*N*,*S* co-ordination mode and, therefore, give rise to separate resonances (δ 8.45, 8.53).

Although the preparation of complexes **3** and **4** was performed in a basic medium (MeOH–NaOMe) the [9]aneS$_3$ ligands retain their facial κ^3*S* co-ordination as truly 'innocent ligands'. This behaviour contrasts with observation of ring opening for the homoleptic complex [Rh([9]aneS$_3$-κ^3*S*)]$^{3+}$ at pH > 4.[3] Addition of 1 molar equivalent of NEt$_3$ leads to deprotonation at a methylene carbon, and subsequent rearrangement of the carbanion affords the vinyl thioether–thiolate complex [Rh{S(CH$_2$)$_2$S(CH$_2$)$_2$SCH=CH$_2$}([9]aneS$_3$-κ^3*S*)]$^{2+}$ *via* C–S bond cleavage. An analogous reactivity has been established for [Co([9]aneS$_3$-κ^3*S*)$_2$]$^{3+}$, [M([9]aneS$_3$-κ^3*S*)$_2$]$^{2+}$ (M = Pd or Pt)[3] and [Ru(η^6-C$_6$Me$_6$)([9]aneS$_3$-κ^3*S*)]$^{2+}$.[6] Indeed it has been suggested that such an irreversible base-induced C–S bond cleavage may be a common feature in the co-ordination chemistry of macrocyclic thioethers and may restrict the extent to which ligands such as [9]aneS$_3$ may be attached to electron-rich transition-metal centres.[6] However, our syntheses of the monocationic ([9]aneS$_3$-κ^3*S*)Rh^{III} complexes **3** and **4** indicate that a relatively high extent of charge neutralization at the metal atom may suppress a C–H activation of the facial [9]aneS$_3$ ligand.

The diethyldithiocarbamate complex **5** exhibits peaks at m/z = 466 and 431 for the molecular ions [M − CF_3SO_3]$^+$ and [M − CF_3SO_3 − Cl]$^+$ in its FAB mass spectrum. Resonances at δ 1.27 and 3.71 in the ^{1}H NMR spectrum belong to the CH_3 and CH_2 protons of the $S_2CNEt_2^-$ ligand. We believed that the energetically favourable κ^2*S*,*S*′ chelate co-ordination of two $S_2CNEt_2^-$ moieties might lead to a κ^2*S* co-ordination mode of the macrocyclic thioether when **1** is treated with 2 molar equivalents of the dialkyldithiocarbamate. Although the reaction product [{Rh(S$_2$CNEt$_2$)$_2$}$_2$-{μ-S(CH$_2$)$_2$S(CH$_2$)$_2$SCH=CH$_2$}$_2$] **6** does, indeed, exhibit two κ^2*S*,*S*′ co-ordinated S_2CNEt_2 ligands at each Rh^{III}, it is apparent that base-induced C–S bond cleavage leads to ring opening of the previously κ^3*S* co-ordinated [9]aneS$_3$. In contrast to [Rh{S(CH$_2$)$_2$S(CH$_2$)$_2$SCH=CH$_2$}([9]aneS$_3$-κ^3*S*)]$^{2+}$ in which the vinyl thioether–thiolate moiety [S$_3$C$_6$H$_{11}$]$^-$ adopts a κ^3*S*,*S*′,*S*″ co-ordination mode,[3] only the thiolate S atoms of the analogous ligands in **6** participate in metal co-ordination (Fig. 4). These atoms bridge two rhodium(III) centres to afford a dinuclear complex with a central (RhS)$_2$ ring and crystallographic C_i symmetry. The planar central (RhS)$_2$ ring displays endocyclic bond angles of

Table 4 Fractional atomic coordinates ($\times 10^4$) with e.s.d.s in parentheses

Atom	*x*	*y*	*z*	Atom	*x*	*y*	*z*
Compound **1**							
Rh	1 345(1)	0	1 987(1)	C(22′)	−1 629(91)	3 152(58)	2 103(102)
Cl	573(4)	−95(25)	−177(4)	S(1′)	4 753(4)	−48(14)	8 144(4)
S(1)	2 820(13)	−1 488(12)	1 961(12)	O(1′)	4 769(29)	−1 286(18)	7 655(25)
S(4)	2 217(4)	2(16)	4 104(3)	O(2′)	3 922(10)	23(25)	8 876(9)
S(7)	2 731(14)	1 505(13)	1 866(12)	O(3′)	4 600(31)	961(22)	7 285(21)
C(2)	3 680(28)	−1 772(27)	3 612(15)	F(1′)	6 529(20)	−856(27)	10 098(19)
C(3)	3 124(30)	−1 458(20)	4 598(24)	F(2′)	7 233(12)	−205(30)	8 667(14)
C(5)	3 524(24)	1 155(22)	4 329(26)	F(3′)	6 586(30)	1 091(23)	9 776(23)
C(6)	3 433(34)	2 182(22)	3 422(17)	C(1′)	6 369(9)	−5(22)	9 215(11)
C(8)	4 008(34)	787(37)	1 379(31)	S(21′)	7 525(7)	−92(14)	4 397(6)
C(9)	4 149(26)	−578(33)	1 736(30)	S(22′)	7 744(23)	113(77)	5 401(24)
N(1)	41(23)	−1 402(22)	1 989(26)	C(2′)	9 049(13)	−38(21)	5 627(15)
C(11)	−730(19)	−2 074(21)	2 073(27)	O(4′)	7 690(15)	279(19)	3 249(11)
C(12)	−1 766(28)	−2 894(28)	2 242(39)	O(5′)	7 061(24)	−1 379(13)	4 278(21)
N(2)	−5(20)	1 305(21)	2 117(27)	O(6′)	6 599(17)	651(15)	4 760(16)
C(21)	−906(27)	1 904(33)	2 009(39)	F(4′)	9 864(24)	−689(20)	5 236(21)
C(21′)	−530(43)	2 185(49)	2 281(50)	F(5′)	9 137(25)	1 193(20)	5 565(22)
C(22)	−1 925(35)	2 824(41)	2 069(41)	F(6′)	8 788(22)	−519(21)	6 569(20)
Compound **2**							
Rh	0	3 867(1)	1 257(1)	C(51)	683(7)	2 678(3)	1 548(8)
B	0	4 950(6)	1 827(8)	C(52)	692(7)	2 738(4)	1 754(7)
N(11)	1 388(8)	4 435(2)	1 129(3)	F(1)	0	802(3)	1 369(4)
N(12)	1 198(9)	4 878(3)	1 432(3)	F(2)	1 003(10)	1 489(3)	1 490(4)
C(13)	2 123(11)	5 209(3)	1 254(5)	C(1′)	0	1 279(4)	1 219(4)
C(14)	2 863(12)	4 987(4)	828(5)	O(1)	1 162(11)	1 134(4)	254(5)
C(15)	2 407(10)	4 499(3)	775(4)	O(2)	0	1 916(3)	353(5)
N(21)	0	4 052(4)	2 169(4)	S(1′)	0	1 390(1)	429(2)
N(22)	0	4 542(4)	2 322(5)	O(41)	5 000	2 678(10)	2 039(11)
C(23)	0	4 581(7)	2 924(7)	O(42)	3 945(18)	2 302(8)	1 113(9)
C(24)	0	4 118(7)	3 170(7)	O(51)	5 000	2 368(10)	903(5)
C(25)	0	3 793(5)	2 678(6)	O(52)	3 836(12)	2 507(6)	1 855(7)
S(1)	0	3 657(1)	254(1)	F(41)	5 000	1 343(9)	1 297(11)
S(4)	1 582(3)	3 270(1)	1 418(1)	F(42)	4 018(17)	1 569(8)	2 119(7)
C(21)	1 198(14)	3 142(6)	177(4)	F(51)	5 000	1 588(8)	2 319(7)
C(22)	1 500(11)	3 285(6)	150(3)	F(52)	4 004(13)	1 457(5)	1 459(6)
C(31)	2 207(12)	3 120(6)	661(3)	S(2′)	5 000	2 329(2)	1 550(2)
C(32)	1 908(16)	2 981(6)	677(4)	C(2′)	5 000	1 672(4)	1 741(7)
Compound **3**							
Rh	6 238(1)	2 494(1)	4 518(1)	C(13)	7 254(13)	4 493(12)	2 420(9)
Cl	5 497(3)	1 091(3)	3 347(2)	C(14)	6 177(14)	5 087(11)	2 149(9)
S(1)	7 042(3)	3 825(3)	5 659(2)	S′	1 149(4)	2 863(4)	4 200(3)
S(4)	5 551(3)	1 543(3)	5 574(2)	O(1′)	2 102(13)	2 533(22)	3 841(14)
S(7)	8 016(3)	1 505(3)	5 066(2)	O(2′)	474(21)	1 919(15)	4 360(14)
C(2)	6 754(13)	3 328(13)	6 728(8)	O(3′)	438(21)	3 794(13)	3 713(13)
C(3)	5 605(13)	2 607(17)	6 453(9)	O(1″)	2 016(12)	2 087(13)	4 043(11)
C(5)	6 825(12)	642(13)	6 240(12)	O(2″)	52(10)	2 356(16)	4 207(11)
C(6)	7 575(13)	338(11)	5 636(10)	O(3″)	1 064(17)	3 819(9)	3 576(9)
C(8)	8 933(10)	2 329(10)	6 081(8)	C′	1 891(7)	3 346(7)	5 398(5)
C(9)	8 623(11)	3 540(11)	5 929(9)	F(1′)	1 175(14)	3 683(18)	5 875(12)
S(11)	4 559(3)	3 674(3)	3 766(2)	F(2′)	2 712(15)	4 114(14)	5 442(12)
N(11)	6 554(8)	3 530(7)	3 494(6)	F(3′)	2 505(18)	2 481(11)	5 901(11)
C(11)	5 538(11)	4 123(10)	3 176(8)	F(1″)	1 219(13)	4 196(13)	5 524(11)
N(12)	5 320(9)	4 893(9)	2 514(7)	F(2″)	2 959(10)	3 768(15)	5 492(11)
C(12)	7 403(12)	3 722(11)	3 093(8)	F(3″)	1 962(17)	2 614(13)	6 088(8)
Compound **6**							
Rh	5 194(1)	302(1)	6 284(1)	S(8)	5 275(1)	463(1)	4 341(3)
S(11)	5 141(1)	72(1)	8 186(3)	C(1)	5 880(5)	640(6)	4 054(11)
S(12)	5 800(1)	144(1)	6 579(3)	C(2)	5 959(4)	691(15)	2 760(17)
C(11)	5 600(5)	1(5)	7 947(11)	C(2′)	5 980(5)	794(14)	2 822(19)
N(11)	5 783(4)	−148(4)	8 696(9)	S(9)	6 580(2)	956(2)	2 500(5)
C(12)	6 167(5)	−227(5)	8 428(12)	C(3)	6 877(9)	1 409(7)	3 537(19)
C(13)	6 626(5)	183(6)	8 765(14)	C(4)	6 913(13)	1 832(9)	2 906(28)
C(14)	5 604(6)	−255(6)	9 867(11)	S(10)	7 230(8)	2 375(8)	3 705(19)
C(15)	5 258(7)	−760(6)	10 009(16)	C(5)	6 863(27)	2 283(32)	4 942(50)
S(21)	4 650(1)	550(1)	6 440(3)	C(61)	6 788(75)	2 626(56)	5 261(144)
S(22)	5 614(1)	1 095(2)	6 764(3)	C(62)	6 409(25)	2 111(66)	4 777(109)
C(21)	5 094(6)	1 080(5)	6 806(12)	C(3′)	6 913(12)	1 583(4)	2 702(28)
N(21)	5 055(5)	1 435(5)	7 122(12)	C(4′)	7 034(13)	1 668(9)	3 958(28)
C(22)	5 463(8)	1 893(7)	7 328(24)	S(10′)	7 282(8)	2 270(8)	4 339(19)
C(23)	5 500(14)	1 945(13)	8 599(25)	C(5′)	6 826(17)	2 407(20)	4 589(94)
C(24)	4 588(7)	1 377(6)	7 277(17)	C(61′)	6 884(55)	2 812(50)	4 214(163)
C(25)	4 537(8)	1 756(7)	6 744(19)	C(62′)	6 937(37)	2 816(42)	5 059(193)

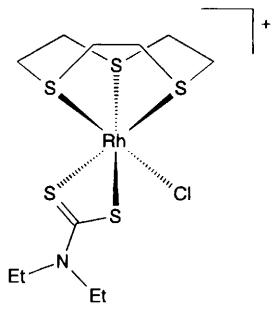

5

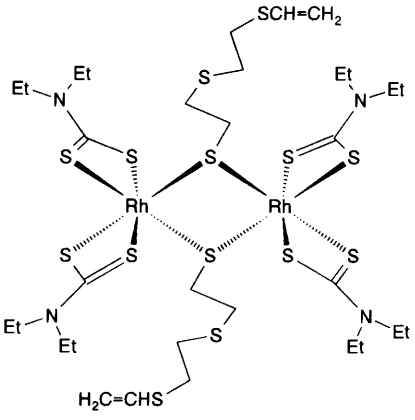

6

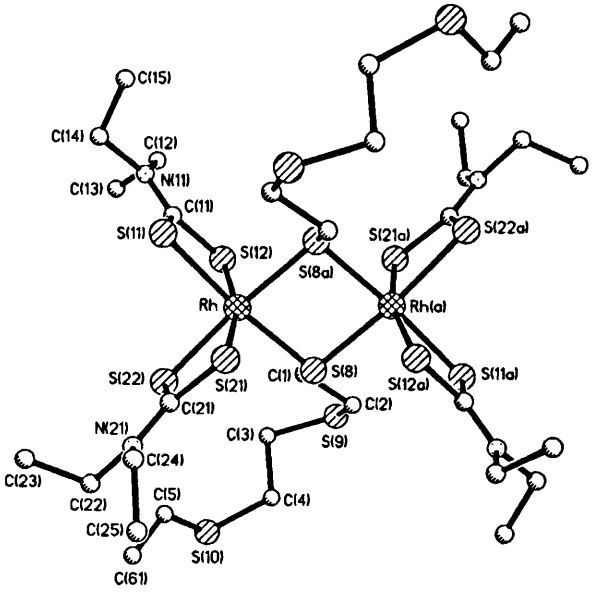

Fig. 4 Molecular structure of $[\{Rh(S_2CNEt_2)_2\}_2\{\mu\text{-}S(CH_2)_2S(CH_2)_2\text{-}SCH{=}CH_2\}_2]$ **6**, showing one possible conformation of the disordered vinyl thioether–thiolate ligand. The depicted atoms C(2)–C(5) and S(10) all exhibit site-occupation factors of 0.5 with the terminal atom capable of adopting two alternative positions C(61) (as depicted) or C(62) (not depicted)

83.1(1) and 96.9(1)° at the Rh and S atoms leading to a transannular Rh · · · Rh distance of 3.524(2) Å. The solid-state structure is fully consistent with the FAB mass and ^{1}H NMR spectroscopic data. Complex **6** exhibits two different fragmentation pathways with peaks at m/z = 1156, 1008, 977 and 829 corresponding to molecular ions M^+, $[M - S_2CNEt_2]^+$, $[M - S_3C_6H_{11}]^+$ and $[M - S_2CNEt_2 - S_3C_6H_{11}]^+$. Proton NMR resonances (CD_3OD) are registered at δ 1.34 and 3.77 for the CH_3 and CH_2 protons of the $S_2CNEt_2^-$ ligand and at δ 5.23 (4 H, CH=CH_2) and 6.44 (2 H, CH=CH_2) for the vinyl protons. Analogous signals at δ 6.2 and 6.6 were recorded for the vinyl protons of $[Rh\{S(CH_2)_2S(CH_2)_2SCH{=}CH_2\}([9]aneS_3\text{-}\kappa^3S)]^{2+}$ in basic aqueous solution.[3]

The present results indicate that $[RhCl(MeCN)_2([9]aneS_3\text{-}\kappa^3S)][CF_3SO_3]_2$ **1** should provide an expedient starting material for the synthesis of a wide range of half-sandwich rhodium(III) complexes. Irreversible base-induced C–S bond cleavage may, however, restrict its range of application.

Acknowledgements

We thank Degussa for a gift of $RhCl_3 \cdot 3H_2O$ and the Fonds der Chemischen Industrie for their financial support of this work.

References

1 S. R. Cooper, *Acc. Chem. Res.*, 1988, **21**, 141; S. R. Cooper and S. C. Rawle, *Struct. Bonding (Berlin)*, 1990, **72**, 1.
2 M. Schröder, *Pure Appl. Chem.*, 1988, **60**, 517; A. J. Blake and M. Schröder, *Adv. Inorg. Chem.*, 1990, **35**, 1.
3 A. J. Blake, A. J. Holder, T. I. Hyde, H.-J. Küppers, M. Schröder, S. Stötzel and K. Wieghardt, *J. Chem. Soc., Chem. Commun.*, 1989, 1600.
4 A. J. Blake, M. A. Halcrow and M. Schröder, *J. Chem. Soc., Chem. Commun.*, 1991, 253.
5 A. J. Blake, R. M. Christie, Y. V. Roberts, M. J. Sullivan, M. Schröder and L. J. Yellowlees, *J. Chem. Soc., Chem. Commun.*, 1992, 848.
6 M. A. Bennett, L. Y. Goh and A. C. Willis, *J. Chem. Soc., Chem. Commun.*, 1992, 1180.
7 A. F. Hill, N. W. Alcock, J. C. Cannadine and G. R. Clark, *J. Organomet. Chem.*, 1992, **426**, C40; J. C. Cannadine, A. Hector and F. Hill, *Organometallics*, 1992, **11**, 2323; N. W. Alcock, J. C. Cannadine, G. R. Clark and A. F. Hill, *J. Chem. Soc., Dalton Trans.*, 1993, 1131.
8 A. J. Blake, R. O. Gould, M. A. Halcrow and M. Schröder, *J. Chem. Soc., Dalton Trans.*, 1994, 2197.
9 C. Landgrafe and W. S. Sheldrick, *J. Chem. Soc., Dalton Trans.*, 1994, 1885.
10 H.-J. Kim, J.-H. Lee, I.-H. Suh and Y. Do, *Inorg. Chem.*, 1995, **34**, 796.
11 G. M. Sheldrick, SHELXTL PLUS programs for use with Siemens X-ray systems, University of Göttingen, 1990.
12 G. M. Sheldrick, SHELXL 93, A Program for Structure Refinement, University of Göttingen, 1993.
13 *International Tables for X-Ray Crystallography*, Kynoch Press, Birmingham, 1974, vol. 4.
14 S. C. Rawle, G. Admans and S. R. Cooper, *J. Chem. Soc., Dalton Trans.*, 1988, 93.
15 N. W. Alcock, N. Herron and P. J. Moore, *J. Chem. Soc., Dalton Trans.*, 1978, 394; *J. Chem. Soc., Chem. Commun.*, 1976, 886.
16 I. R. Young, L. A. Ochrymowycz and D. B. Rorabacher, *Inorg. Chem.*, 1986, **25**, 2576; L. S. W. L. Sokol, L. A. Ochrymowycz and D. B. Rorabacher, *Inorg. Chem.*, 1981, **20**, 3189.
17 D. Rogers, *Acta Crystallogr., Sect. A*, 1981, **37**, 734.
18 S. Trofimenko, *Acc. Chem. Res.*, 1971, **4**, 17.
19 A. M. McNair, D. C. Boyd and K. R. Mann, *Organometallics*, 1986, **5**, 303.
20 S. May, P. Reinsake and J. Powell, *Inorg. Chem.*, 1980, **19**, 1582; J. S. Thompson, R. L. Harlow and J. F. Whitney, *J. Am. Chem. Soc.*, 1983, **105**, 3522.
21 S. C. Rawle, R. Yagbasan, K. Prout and S. R. Cooper, *J. Am. Chem. Soc.*, 1987, **109**, 6181; S. R. Cooper, S. C. Rawle, R. Yagbasan and D. J. Watkin, *J. Am. Chem. Soc.*, 1991, **113**, 1600.
22 H.-J. Kim, J. H. Jeong and Y. Do, *Bull. Korean Chem. Soc.*, 1992, **13**, 463.
23 C. Landgrafe and W. S. Sheldrick, unpublished work.
24 E. S. Raper, *Coord. Chem. Rev.*, 1985, **61**, 115.
25 W. S. Sheldrick and C. Landgrafe, *Inorg. Chim. Acta*, 1993, **208**, 145.

Received 17*th August* 1995; *Paper* 5/05491E